Fredkin Staircase: An Integrable System with a Finite-Frequency Drude Peak

Hansveer Singh,[1] Romain Vasseur,[1] and Sarang Gopalakrishnan[2,3]
[1]Department of Physics, University of Massachusetts, Amherst, Massachusetts 01003, USA
[2]Department of Physics, Pennsylvania State University, University Park Pennsylvania 16802, USA
[3]Department of Electrical and Computer Engineering, Princeton University, Princeton New Jersey 08544, USA

(Received 21 June 2022; revised 8 January 2023; accepted 10 January 2023; published 27 January 2023)

We introduce and explore an interacting integrable cellular automaton, the Fredkin staircase, that lies outside the existing classification of such automata, and has a structure that seems to lie beyond that of any existing Bethe-solvable model. The Fredkin staircase has two families of ballistically propagating quasiparticles, each with infinitely many species. Despite the presence of ballistic quasiparticles, charge transport is diffusive in the dc limit, albeit with a highly non-Gaussian dynamic structure factor. Remarkably, this model exhibits persistent temporal oscillations of the current, leading to a delta-function singularity (Drude peak) in the ac conductivity *at nonzero frequency*. We analytically construct an extensive set of operators that anticommute with the time-evolution operator; the existence of these operators both demonstrates the integrability of the model and allows us to lower bound the weight of this finite-frequency singularity.

DOI: 10.1103/PhysRevLett.130.046001

Introduction.—In conventional metals, the optical conductivity has a peak at zero frequency with a width set by the mean free time. This zero-frequency peak is called the "Drude peak" and becomes sharp in the limit of low temperatures or weak interactions. Recently, motivated by experiments on bad metals [1,2], there has been considerable interest in systems that have *finite-frequency* Drude peaks [3–7]. Attempts have been made to model these in terms of imperfect Anderson localization [4] and fluctuating density waves [6]; such explanations yield a *broad* maximum: the peak frequency and the width of the peak are set by the same scale. To our knowledge, no model has been shown to have both an O(1) dc resistance and a *sharp* finite-frequency Drude peak.

In the present work we construct an exactly solvable model with these features. This model is an interacting integrable cellular automaton, with an update rule analogous to the Fredkin model which we dub the Fredkin staircase automaton (FSA) [8,9]. The Fredkin model is one of a large class of kinetically constrained models (KCMs) that have recently been explored and shown to exhibit anomalous dynamical properties [10–21]. Remarkably, there are deep links between integrable systems and KCMs: if one applies the update rules of a KCM in certain deterministic sequences (rather than at random) one obtains discrete-time integrable cellular automata. This correspondence has been noted in multiple cases (see, e.g., Refs. [22–32]); how general it is, and how the properties of the stochastic and integrable versions of the model are related, remain open questions.

We show that the FSA is integrable—we can construct extensively many conserved quantities, and identify stable quasiparticles. Remarkably, our simulations of scattering events between quasiparticles suggest that, despite its integrability, the FSA does not fit the standard Bethe ansatz paradigm, and hence evades exact solvability at present. Whether the Bethe ansatz framework can be extended to the FSA is an important topic for future work.

After discussing the quasiparticle structure, we study transport in this model by numerically computing its ac conductivity through the Kubo formula [33]. Our central result is that the ac conductivity has an infinitely sharp (i.e., δ-function) "Drude" peak at a *nonzero* frequency, associated with persistent oscillations of current fluctuations. We are unaware of any other integrable systems with a nonzero-frequency Drude peak. We explain this finite-frequency Drude peak in terms of an infinite family of charges that *anticommute* with the time evolution operator. In terms of these charges, we derive an analytic lower bound for the weight of the Drude peak. In addition to this feature, the dc limit of the conductivity is finite, so transport is asymptotically diffusive despite the presence of ballistic quasiparticles. This peculiar phenomenon has been observed and explained in the context of the easy-axis XXZ spin chain [34–38]; remarkably it also occurs in this model although its transport properties are otherwise very different. In contrast to the XXZ spin chain, although the FSA exhibits diffusion, its dynamical structure factor is spatially strongly asymmetric, and obeys a scaling form $C(x,t) = t^{-1/z} f(x/t^{1/z})$, with $z = 2$ and f a skewed, non-Gaussian scaling function.

Model.—Our system is a one-dimensional chain of qubits of length L whose basis states we represent as $|\bullet\rangle$ and $|\circ\rangle$ to denote whether a particle has occupied a site or

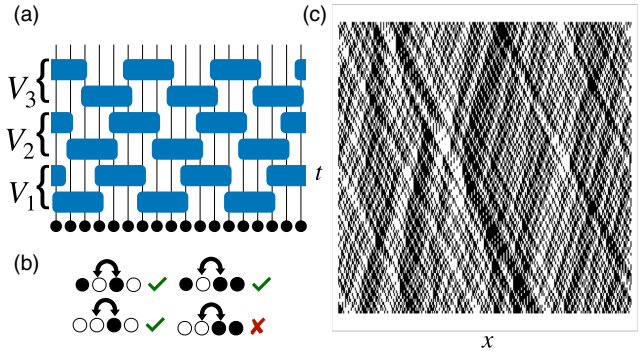

FIG. 1. Model. (a) Pictorial representation of the circuit geometry described by Eq. (1). (b) Pictorial representation of the rules associated to the Fredkin constraint as described in Eq. (2). • represents particles while ◦ represents holes. (c) Time evolution of a random product state in the occupation basis.

not. The dynamics is governed by a Floquet operator $\mathcal{U}$, shown pictorially in Fig. 1, which is composed of three layers of four site unitary gates, i.e., $\mathcal{U} = V_3 V_2 V_1$, where

$$V_i = \prod_{j \equiv i \bmod 3} U_{j,j+1,j+2,j+3}, \tag{1}$$

and

$$\begin{aligned} U_{j,j+1,j+2,j+3} = {} & P^{\bullet}_j \mathrm{SWAP}_{j+1,j+2} P^{\bullet} \\ & + P^{\bullet}_j \mathrm{SWAP}_{j+1,j+2} P^{\circ}_{j+3} \\ & + P^{\circ}_j \mathrm{SWAP}_{j+1,j+2} P^{\circ}_{j+3} \\ & + P^{\circ}_j \mathbb{1}_{j+1,j+2} P^{\bullet}_{j+3}. \end{aligned} \tag{2}$$

$P^{\bullet}_j = |\bullet\rangle\langle\bullet|_j$, $P^{\circ}_j = |\circ\rangle\langle\circ|_j$ and $\mathrm{SWAP}_{j,j+1}$ is the usual SWAP gate. Note that these gates locally preserve particle number so that the total particle number of the system is conserved. By inspection, one can see that the Floquet operator is invariant under translation by three sites; thus we break our system into three site unit cells. This gate geometry was first used (but with different gates) in Ref. [27], and one can show that the gate geometry is equivalent to a staircase geometry, hence the name Fredkin staircase automaton, as the constrained swaps satisfy the so-called Fredkin constraint [39–49]. We note that the gate pattern we are using is crucial for the model to be integrable. In the Supplemental Material [50], we show that deforming the gate geometry breaks the integrability of the model and leads to subdiffusion with an exponent $z \simeq 8/3$ in line with the predictions of Ref. [8]. Each update conserves the total number of • (and ◦) sites, so we can regard the fraction of • sites as the "filling fraction" f.

Quasiparticles.—We first identify single quasiparticle excitations of the FSA model above its vacuum state (i.e., the state $|\circ\rangle^{\otimes N}$). One can create states with a single elementary quasiparticle by occupying a single site.

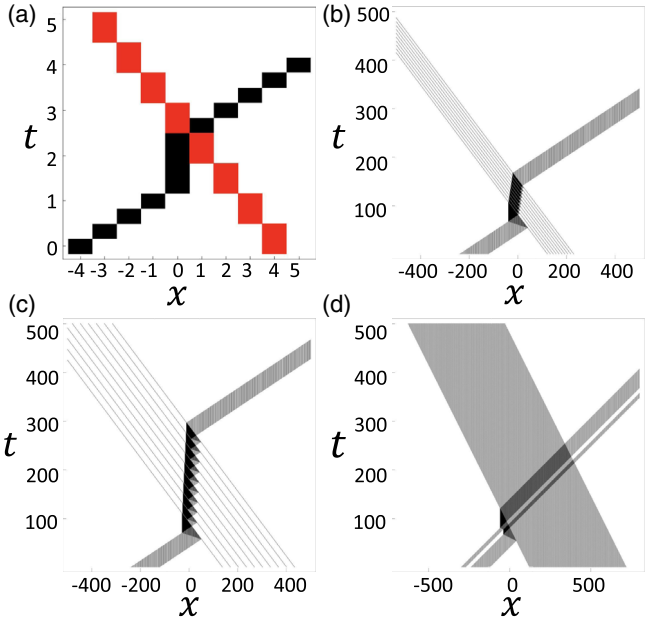

FIG. 2. Quasiparticles scattering. (a) A collision between a single σ (colored red) and β (colored black) quasiparticle where integer time steps represent evolving by a full Floquet step while fractional steps indicate evolving by individual layers. One can see the σ particle receives no scattering shift, but the β particle is delayed by one Floquet time step. (b) A β string of (moving right) collides with 10σ quasiparticles consecutively spaced by two unit cells (moving left). One can clearly see that the velocity of the β string is renormalized when it passes through the σ quasiparticles. (c) A size 40β string collides with ten σ quasiparticles consecutively spaced by ten unit cells. Observe that the β string's velocity is much lower than compared with the previous situation indicating that the effective velocity of β strings is highly dependent on spacings of σ quasiparticles. (d) Two β strings collide when they encounter the large number of σ particles. One can see that the smaller β-string overtakes the larger one after the collision occurs.

Since there are three inequivalent sites in the unit cell there are three inequivalent quasiparticles [50]. For the gate pattern and unit cell in Fig. 1, quasiparticles on the first and third sites of the unit cell move ballistically leftward with velocity $v_\sigma = 3/2$, shown in red in Fig. 2, whereas those on the second site move rightward with velocity $v_\beta = 3$, shown in black in Fig. 2—as this notation anticipates we will call the two left-moving quasiparticles σ quasiparticles and the right-moving quasiparticle a β quasiparticle. (We will avoid calling them left and right movers as the direction they move is set by the arbitrarily chosen chirality of the gate pattern.)

We now turn to the scattering between quasiparticles. Here, in contrast to standard integrable systems, we find a strong asymmetry between σ and β quasiparticles: the trajectories of σ quasiparticles are totally unaffected by collisions, while β quasiparticles are slowed down. When colliding with a single σ quasiparticle, a sequence of s β

quasiparticles is slowed down by s unit cells. These sequences thus form collectively moving bound states, which we call β strings of size s. Collisions with σ quasiparticles renormalize the velocities of such β strings in an s-dependent way. Because β strings of different sizes have different renormalized velocities (in the presence of σ strings), two β strings can collide (when a smaller string overtakes a larger one), as in the bottom-right panel of Fig. 2. When two β strings of size (s, s') collide the faster of them is further sped up (and the slower is further slowed down) by $2\ \min(s, s')$ unit cells. This scattering phase shift precisely parallels the result for Heisenberg and XXZ spin chains. We note that all the observations that we have made regarding scattering have been empirically deduced from the numerics. It would be interesting to construct an analytical proof for these statements as well as further investigate why the scattering shift of β strings parallels that of the Heisenberg and XXZ spin chains.

To set up generalized hydrodynamics for this model, we would need the scattering shifts between an arbitrary-size β string and an arbitrary configuration of σ quasiparticles. In a typical Bethe-ansatz solvable problem, the σ quasiparticles would form some set of bound states or "σ strings," and the scattering shift accumulated by a β string passing through the σ quasiparticles would be a sum of shifts due to each σ-type string. In the FSA this separation does not happen: rather, the scattering shift is sensitive to the full pattern of spacings between σ quasiparticles (Fig. 2). Thus, from the point of view of their scattering properties, even two arbitrarily well separated σ quasiparticles cannot be treated as independent scatterers with additive scattering shifts. Although we are able to find expressions for the scattering shift of an arbitrary β string in an arbitrary background of σ quasiparticles, it is not clear how to express these in the standard Bethe ansatz form. Nevertheless, our numerical results strongly suggest that all quasiparticles are stable (so the model is integrable), and we now explicitly demonstrate this for the σ quasiparticles.

Integrability.—In this section we show that there are an infinite number of quasilocal operators that are conserved. The construction relies on the observation that evolution by one Floquet step maps $P^{\bullet}_{3x+1}P^{\circ}_{3x+3}$ to $P^{\bullet}_{3x}P^{\circ}_{3x+1}$ and maps $P^{\bullet}_{3x}P^{\circ}_{3x+1}$ to $P^{\bullet}_{3x-2}P^{\circ}_{3x}$ (we use the convention that the index of the first site in the unit cell has the form $3j+1$). Intuitively the evolution of these projectors corresponds to a σ quasiparticle propagating to the left. One can construct a number operator counting the total number of σ quasiparticles spaced by s unit cells, and it is given by

$$N_s = N_s^A + N_s^B, \tag{3}$$

where

$$N_s^{A/B} = \sum_{x=0}^{L/3-1} P_x^{A/B} \prod_{y=1}^{s} (\mathbb{1} - P_{x+y}^{A/B}) P_{x+s+1}^{A/B}, \qquad s > 0 \tag{4}$$

$$N_0^{A/B} = \sum_{x=0}^{L/3-1} P_x^{A/B} P_{x+1}^{A/B}, \tag{5}$$

where $P_x^A = P^{\bullet}_{3x+1}P^{\circ}_{3x+3}$ and $P_x^B = P^{\bullet}_{3x}P^{\circ}_{3x+1}$. We note that the $N_s^{A/B}$ correspond to the asymptotic spacings [35] of the σ quasiparticles.

One can see that N_s is conserved since the Floquet operator maps P_x^A to P_x^B and P_x^B to P_{x-1}^A. All operators commute with each other since they are diagonal in the occupation basis. Additionally, they are orthogonal to each other under the Hilbert-Schmidt inner product (i.e., $\langle A, B\rangle \equiv 2^{-L}\langle A^{\dagger}B\rangle$) because for $s' > s$, all terms in $N_{s'}$ have larger support than all terms in N_s. Since we constructed an infinite set of linearly independent conserved quasilocal operators, the FSA model is integrable. We note that there are clearly more operators which are conserved such as the total number of β strings. It would be interesting to further investigate the algebraic integrable structure of this model in future work [26–29,54,55].

Transport.—Because of its integrability, it is natural to expect particle transport in the FSA model to be ballistic: if the particle current overlaps with any of the conserved charges, it cannot fully relax leading to persistent currents. In what follows, we argue analytically and numerically that transport in the FSA is a lot more exotic and interesting: none of the charges uncovered above overlap with the current operator, and we find numerically that low frequency transport is *diffusive*. However, we identify analytically another set of changes which *anticommute* with the time evolution operator, and which do have a finite overlap with the current. We argue that this leads to a finite Drude peak in the conductivity at frequency $\omega = \pi$. Alternatively, it shows that the FSA is a (fine-tuned) equilibrium discrete *time-crystal* [56–59], as it exhibits persistent oscillating currents.

We characterize the transport properties of the FSA by computing the current-current correlation function, $C_{JJ}(t) = (1/L)\langle J(t)J(0)\rangle$, where $J(t) = \sum_x j(x,t)$ and $j(x,t)$ represents the local current density and $\langle A\rangle \equiv 2^{-L}\mathrm{tr}(A)$ for an operator A. We present the details of the calculation of $j(x,t)$ and its lengthy expression in the Supplemental Material [50]. We numerically computed $C_{JJ}(t)$ using classical evolution, and averages are performed over 10^8 random initial states.

From the current-current correlator, we compute the ac conductivity $\sigma(\omega)$ by using the Kubo formula [33]

$$\sigma(\omega) = \frac{1}{2}C_{JJ}(t=0) + \sum_{t=1}^{\infty} e^{i\omega t} C_{JJ}(t). \tag{6}$$

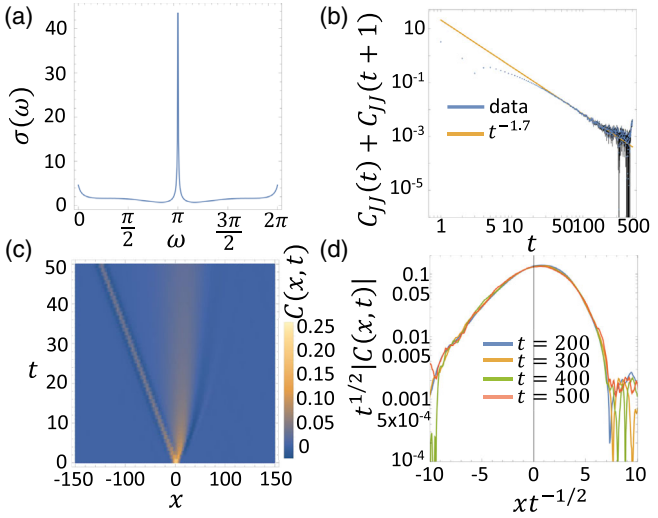

FIG. 3. Transport. (a) ac conductivity $\sigma(\omega)$. Note that $\omega = \pi$ features a prominent peak indicating a π Drude weight and that we also have a finite nonzero value at $\omega = 0$ which suggests diffusive behavior. (b) Behavior of the Kubo correlator $C_{JJ}(t) + C_{JJ}(t+1)$ which is twice the average value over one period of the oscillations in the current-current correlator. $C_{JJ}(t) + C_{JJ}(t+1)$ falls off in a power law fashion, i.e., $t^{-\beta}$, with $\beta \approx 1.7 > 1$ indicating the presence of a finite nonzero diffusion constant at low frequency. (c) Behavior of the particle structure factor $C(x,t)$ at short times and (d) Diffusive scaling collapse of the structure factor, $C(x,t) = t^{-1/2} f(x/t^{1/2})$ with f a non-Gaussian skewed scaling function. (a) and (b) are data averaged over 10^8 realizations, and (c) and (d) are averaged over 10^7 realizations.

Because of the Floquet (discrete time) nature of the model, we have $\omega \in [0, 2\pi)$. We computed this conductivity numerically; see Fig. 3. One can see a clear peak at $\omega = \pi$ indicating persistent oscillations in the time-dependent conductivity and hence also the current-current correlator. We attribute these persistent oscillations to the existence of an extensive number of operators Q such that $\mathcal{U}^\dagger Q \mathcal{U} = -Q$. To see that such operators imply such persistent oscillations, consider the π-Drude weight, defined as

$$\mathcal{D}_\pi = \lim_{t\to\infty} \frac{1}{t} \sum_{\tau=1}^{t} (-1)^\tau C_{JJ}(\tau). \tag{7}$$

The π-Drude weight characterizes the weight of a possible Drude (delta function) peak in the conductivity at frequency π.

One can show that if a collection of operators Q_s satisfy the aforementioned conditions then one can lower bound $\mathcal{D}_\pi$ through the application of a Mazur bound [60–62], i.e.,

$$\mathcal{D}_\pi \geq \frac{3}{L} \sum_s \frac{\langle J(0) Q_s \rangle^2}{\langle Q_s^2 \rangle}. \tag{8}$$

A family of such operators are $Q_s = N_s^A - N_s^B$. Since $\mathcal{U}$ evolves N_s^A to N_s^B at each time step we have

$$\{Q_s, \mathcal{U}\} = 0. \tag{9}$$

We remark that if these were all the charges which anticommuted with $\mathcal{U}$ then Eq. (8) would become an equality. The fact that $\langle J(0) Q_s \rangle \neq 0$ means that $\mathcal{D}_\pi$ is nonzero which implies that $C_{JJ}(t)$ necessarily has to be of the form $C_{JJ}(t) = (-1)^t (\mathcal{D}_\pi + \text{subleading terms})$. Such persistent oscillations indicate that the FSA is a discrete time crystal—albeit fine-tuned rather than generic [56–59,63].

Despite this exotic behavior near $\omega = \pi$ frequency, low-frequency transport appears to be diffusive. None of the charges [Eq. (4)] overlap the current, so there is no obvious zero-frequency Drude weight. Numerically, we find that the averaged Kubo correlators $C_{JJ}(t) + C_{JJ}(t+1)$ decay as $t^{-\beta}$, with an exponent $\beta \approx 1.7 > 1$, indicating a finite dc conductivity $\sigma(\omega = 0)$, and thus a finite diffusion constant. The structure factor $C(x,t) = \langle q(x,t) q(0,0) \rangle$, with q the local particle number appropriately coarse grained over unit cells [50], displays an ever richer structure (Fig. 3), with some ballistic peak (shown in the bottom left panel of Fig. 3) carrying vanishing weight due to σ strings, and an asymmetric non-Gaussian diffusive peak near the origin. This is drastically different from nonintegrable versions of the model where one sees subdiffusive scaling and a symmetric structure factor [8,50].

Discussion.—In this Letter, we introduced a new reversible cellular automaton based on the Fredkin update rule. We showed that the spectrum of this automaton contains two genera of stable quasiparticles, the β strings and the σ quasiparticles. The β strings of all sizes have the same bare velocity, but are renormalized differently through their collisions with σ quasiparticles. Thus this model features an infinite hierarchy of quasiparticles with distinct effective velocities above a typical thermal state. The motion of the σ quasiparticles, meanwhile, is unaffected by the scattering, so it is not entirely clear if (and how) one can assign them to "strings." As we discussed, the β-σ scattering depends nontrivially on the spacing between adjacent σ quasiparticles; while this dependence can be computed, we have not been able to factor it into contributions due to a hierarchy of σ-type strings. Thus the full Bethe ansatz solution of this model remains a task for future work. We remark that this model does not appear to fall under a current partial classification of integrable cellular automatons [28,64].

Although we were unable to fully solve the model, we could analytically establish the presence of an infinite hierarchy of conserved charges; physically, these charges represent the spacings between σ quasiparticles, which are conserved. Such asymptotic spacings are also conserved in the Rule 54 reversible cellular automaton [23,26] but do not seem to affect the hydrodynamics of the model. However,

scattering of β strings depends on spacings of σ particles in a σ string suggesting that they might play a role in determining the late time behavior of the FSA.

Finally, we studied transport properties in this model. We found that the dc limit of transport is diffusive, but with an asymmetric and non-Gaussian dynamic structure factor. Moreover, the model features persistent current oscillations, leading to a finite-frequency delta-function peak in the ac conductivity. A comprehensive understanding of the transport behavior in this model should be amenable to generalized hydrodynamics [51]. However, this would require one to re-express the scattering data in a standard Bethe-ansatz form; this task is currently out of reach.

We thank B. Pozsgay and B. Ware for stimulating discussions. This work was supported by the National Science Foundation under NSF Grant No. DMR-1653271 (S. G.), the U.S. Department of Energy, Office of Science, Basic Energy Sciences, under Early Career Award No. DE-SC0019168 (R. V.), and the Alfred P. Sloan Foundation through a Sloan Research Fellowship (R. V.).

[1] O. Gunnarsson, M. Calandra, and J. Han, Colloquium: Saturation of electrical resistivity, Rev. Mod. Phys. **75**, 1085 (2003).
[2] S. Caprara, C. Di Castro, S. Fratini, and M. Grilli, Anomalous Optical Absorption in the Normal State of Overdoped Cuprates Near the Charge-Ordering Instability, Phys. Rev. Lett. **88**, 147001 (2002).
[3] S. Fratini, D. Mayou, and S. Ciuchi, The transient localization scenario for charge transport in crystalline organic materials, Adv. Funct. Mater. **26**, 2292 (2016).
[4] S. Fratini and S. Ciuchi, Displaced drude peak and bad metal from the interaction with slow fluctuations., SciPost Phys. **11**, 039 (2021).
[5] G. Masella, N. V. Prokof'ev, and G. Pupillo, Anti-drude metal of bosons, Nat. Commun. **13**, 2113 (2022).
[6] L. Delacrétaz, B. Goutéraux, S. Hartnoll, and A. Karlsson, Bad metals from fluctuating density waves, SciPost Phys. **3**, 025 (2017).
[7] J. Kokalj, Bad-metallic behavior of doped Mott insulators, Phys. Rev. B **95**, 041110 (2017).
[8] H. Singh, B. A. Ware, R. Vasseur, and A. J. Friedman, Subdiffusion and Many-Body Quantum Chaos with Kinetic Constraints, Phys. Rev. Lett. **127**, 230602 (2021).
[9] L. Causer, J. P. Garrahan, and A. Lamacraft, Slow dynamics and large deviations in classical stochastic Fredkin chains, Phys. Rev. E **106**, 014128 (2022).
[10] J. P. Garrahan, Aspects of non-equilibrium in classical and quantum systems: Slow relaxation and glasses, dynamical large deviations, quantum non-ergodicity, and open quantum dynamics, Physica (Amsterdam) **504A**, 130 (2018).
[11] G. H. Fredrickson and H. C. Anderson, Kinetic Ising Model of the Glass Transition, Phys. Rev. Lett. **53**, 1244 (1984).
[12] J. P. Garrahan, P. Sollich, and C. Toninelli, Kinetically constrained models, arXiv:1009.6113v1.
[13] F. Ritort and P. Sollich, Glassy dynamics of kinetically constrained models, Adv. Phys. **52**, 219 (2003).
[14] B. Everest, M. Marcuzzi, J. Garrahan, and I. Lesanovsky, Emergent kinetic constraints, ergodicity breaking, and cooperative dynamics in noisy quantum systems, Phys. Rev. E **94**, 052108 (2016).
[15] J. Iaconis, S. Vijay, and R. Nandkishore, Anomalous subdiffusion from subsystem symmetries, Phys. Rev. B **100**, 214301 (2019).
[16] J. Feldmeier, P. Sala, G. D. Tomasi, F. Pollmann, and M. Knapp, Anomalous Diffusion in Dipole- and Higher-Moment-Conserving Systems, Phys. Rev. Lett. **125**, 245303 (2020).
[17] A. Gromov, A. Lucas, and R. Nandkishore, Fracton hydrodynamics, Phys. Rev. Res. **2**, 033124 (2020).
[18] A. Morningstar, V. Khemani, and D. A. Huse, Kinetically constrained freezing transition in a dipole-conserving system, Phys. Rev. B **101**, 214205 (2020).
[19] E. Guardado-Sanchez, A. Morningstar, B. M. Spar, P. T. Brown, D. A. Huse, and W. S. Bakr, Subdiffusion and Heat Transport in a Tilted Two-Dimensional Fermi-Hubbard System, Phys. Rev. X **10**, 011042 (2020).
[20] P. Sala, T. Rakovszky, R. Verresen, M. Knap, and F. Pollmann, Ergodicity Breaking Arising from Hilbert Space Fragmentation in Dipole-Conserving Hamiltonians, Phys. Rev. X **10**, 011047 (2020).
[21] V. Khemani, M. Hermele, and R. Nandkishore, Localization from Hilbert space shattering: From theory to physical realizations, Phys. Rev. B **101**, 174204 (2020).
[22] M. Medenjak, K. Klobas, and T. Prosen, Diffusion in Deterministic Interacting Lattice Systems, Phys. Rev. Lett. **119**, 110603 (2017).
[23] S. Gopalakrishnan, Operator growth and eigenstate entanglement in an interacting integrable Floquet system, Phys. Rev. B **98**, 060302 (2018).
[24] S. Gopalakrishnan and B. Zakirov, Facilitated quantum cellular automata as simple models with non-thermal eigenstates and dynamics, Quantum Sci. Technol. **3**, 044004 (2018).
[25] A. J. Friedman, S. Gopalakrishnan, and R. Vasseur, Integrable Many-Body Quantum Floquet-Thouless Pumps, Phys. Rev. Lett. **123**, 170603 (2019).
[26] B. Buča, K. Klobas, and T. Prosen, Rule 54: Exactly solvable model of nonequilibrium statistical mechanics, J. Stat. Mech. (2021) 074001.
[27] B. Pozsgay, A Yang–Baxter integrable cellular automaton with a four site update rule, J. Phys. A **54**, 384001 (2021).
[28] T. Gombor and B. Pozsgay, Integrable spin chains and cellular automata with medium-range interaction, Phys. Rev. E **104**, 054123 (2021).
[29] T. Gombor and B. Pozsgay, Superintegrable cellular automata and dual unitary gates from Yang-Baxter maps, SciPost Phys. **12**, 102 (2022).
[30] T. Iadecola and S. Vijay, Nonergodic quantum dynamics from deformations of classical cellular automata, Phys. Rev. B **102**, 180302(R) (2020).
[31] J. W. Wilkinson, K. Klobas, T. Prosen, and J. P. Garrahan, Exact solution of the Floquet-PXP cellular automaton, Phys. Rev. E **102**, 062107 (2020).

[32] J. W. P. Wilkinson, T. Prosen, and J. P. Garrahan, Exact solution of the "Rule 150" reversible cellular automaton, Phys. Rev. E **105**, 034124 (2022).
[33] B. Bertini, F. Heidrich-Meisner, C. Karrasch, T.Prosen, R. Steinigeweg, and M. Žnidarič, Finite-temperature transport in one-dimensional quantum lattice models, Rev. Mod. Phys. **93**, 025003 (2021).
[34] J. De Nardis, D. Bernard, and B. Doyon, Hydrodynamic Diffusion in Integrable Systems, Phys. Rev. Lett. **121**, 160603 (2018).
[35] S. Gopalakrishnan, D. A. Huse, V. Khemani, and R. Vasseur, Hydrodynamics of operator spreading and quasiparticle diffusion in interacting integrable systems, Phys. Rev. B **98**, 220303 (2018).
[36] S. Gopalakrishnan and R. Vasseur, Kinetic Theory of Spin Diffusion and Superdiffusion in *xxz* Spin Chains, Phys. Rev. Lett. **122**, 127202 (2019).
[37] J. D. Nardis, D. Bernard, and B. Doyon, Diffusion in generalized hydrodynamics and quasiparticle scattering, SciPost Phys. **6**, 49 (2019).
[38] V. B. Bulchandani, S. Gopalakrishnan, and E. Ilievski, Superdiffusion in spin chains, J. Stat. Mech. (2021) 084001.
[39] L. Dell'Anna, O. Salberger, L. Barbiero, A. Trombettoni, and V. E. Korepin, Violation of cluster decomposition and absence of light cones in local integer and half-integer spin chains, Phys. Rev. B **94**, 155140 (2016).
[40] X. Chen, E. Fradkin, and W. Witczak-Krempa, Gapless quantum spin chains: Multiple dynamics and conformal wavefunctions, J. Phys. A **50**, 464002 (2017).
[41] X. Chen, E. Fradkin, and W. Witczak-Krempa, Quantum spin chains with multiple dynamics, Phys. Rev. B **96**, 180402 (2017).
[42] K. Adhikari and K. S. D. Beach, Slow dynamics of the Fredkin spin chain, Phys. Rev. B **104**, 115149 (2021).
[43] T. Udagawa and H. Katsura, Finite-size gap, magnetization, and entanglement of deformed Fredkin spin chain, J. Phys. A **50**, 405002 (2017).
[44] Z. Zhang and I. Klich, Entropy, gap and a multi-parameter deformation of the Fredkin spin chain, J. Phys. A **50**, 425201 (2017).
[45] O. Salberger and V. Korepin, Fredkin spin chain (2016).
[46] X. Chen, R. Nandkishore, and A. Lucas, Quantum butterfly effect in polarized Floquet systems, Phys. Rev. B **101**, 064307 (2020).
[47] R. Movassagh and P. W. Shor, Supercritical entanglement in local systems: Counterexample to the area law for quantum matter, Proc. Natl. Acad. Sci. U.S.A. **113**, 13278 (2016).
[48] O. Salberger, T. Udagawa, Z. Zhang, H. Katsura, I. Klich, and V. Korepin, Deformed Fredkin spin chain with extensive entanglement, J. Stat. Mech. (2017) 063103.
[49] C. M. Langlett and S. Xu, Hilbert space fragmentation and exact scars of generalized Fredkin spin chains, Phys. Rev. B **103**, L220304 (2021).
[50] See Supplemental Material at http://link.aps.org/supplemental/10.1103/PhysRevLett.130.046001 which includes Refs. [51–53], for details on quasiparticle scattering, details of numerical simulations as well as formulas for the current.
[51] A. Bastianello, B. Bertini, B. Doyon, and R. Vasseur, Introduction to the special issue on emergent hydrodynamics in integrable many-body systems, J. Stat. Mech. (2022) 014001.
[52] U. Schollwöck, The density-matrix renormalization group in the age of matrix product states, Ann. Phys. (Amsterdam) **326**, 96 (2011).
[53] G. M. Crosswhite, Finite automata for caching in matrix product algorithms, Phys. Rev. A **78**, 012356 (2008).
[54] T. Prosen, Reversible cellular automata as integrable interactions round-a-face: deterministic, stochastic, and quantized, arXiv:2106.01292.
[55] T. Gombor and B. Pozsgay, Integrable deformations of superintegrable quantum circuits, arXiv:2205.02038.
[56] V. Khemani, A. Lazarides, R. Moessner, and S. Sondhi, Phase Structure of Driven Quantum Systems, Phys. Rev. Lett. **116**, 250401 (2016).
[57] D. V. Else, B. Bauer, and C. Nayak, Floquet Time Crystals, Phys. Rev. Lett. **117**, 090402 (2016).
[58] V. Khemani, R. Moessner, and S. L. Sondhi, A brief history of time crystals, arXiv:1910.10745.
[59] M. Medenjak, B. Buča, and D. Jaksch, Isolated Heisenberg magnet as a quantum time crystal, Phys. Rev. B **102**, 041117(R) (2020).
[60] P. Mazur, Non-ergodicity of phase functions in certain systems, Physica (Amsterdam) **43**, 533 (1969).
[61] A. Dhar, A. Kundu, and K. Saito, Revisiting the Mazur bound and the Suzuki equality, Chaos, Solitons and Fractals **144**, 110618 (2021).
[62] D. Ampelogiannis and B. Doyon, Ergodicity and hydrodynamic projections in quantum spin lattices at all frequencies and wavelengths, arXiv:2112.12747.
[63] B. Buča, Out-of-Time-Ordered Crystals and Fragmentation, Phys. Rev. Lett. **128**, 100601 (2022).
[64] B. Pozsgay (private communication).